

IDENTIFYING NEAR EARTH OBJECT FAMILIES

HAI FU, ROBERT JEDICKE

Institute for Astronomy, University of Hawaii
2680 Woodlawn Drive, Honolulu, HI, 96822

DANIEL D. DURDA

Southwest Research Institute
1050 Walnut Street Suite 400, Boulder, CO, 80302

AND

RONALD FEVIG, JAMES V. SCOTTI

Lunar and Planetary Lab, University of Arizona
P.O. Box 210092, Tucson, AZ, 85721-0092
accepted for publication in Icarus

ABSTRACT

The study of asteroid families has provided tremendous insight into the forces that sculpted the main belt and continue to drive the collisional and dynamical evolution of asteroids. The identification of asteroid families within the NEO population could provide a similar boon to studies of their formation and interiors. In this study we examine the purported identification of NEO families by Drummond (2000) and conclude that it is unlikely that they are anything more than random fluctuations in the distribution of NEO osculating orbital elements. We arrive at this conclusion after examining the expected formation rate of NEO families, the identification of NEO groups in synthetic populations that contain no genetically related NEOs, the orbital evolution of the largest association identified by Drummond (2000), and the decoherence of synthetic NEO families intended to reproduce the observed members of the same association. These studies allowed us to identify a new criterion that can be used to select real NEO families for further study in future analyses, based on the ratio of the number of *pairs* and the size of *strings* to the number of objects in an identified *association*.

Subject headings: asteroids, dynamics

1. INTRODUCTION

The discovery of a group of Near Earth Objects (NEO) that all derive from the products of a catastrophically disrupted NEO parent body would be an important step in understanding their structure and dynamical evolution. It would be equivalent to the information afforded a geologist in cracking open a rock with a hammer. Studies of the chips off the old block of a larger asteroid will provide interesting insights, just as the study of similarly formed main belt (MB) asteroid families has provided critical information to the study of those asteroids (*e.g.*, Cellino et al. 2004; Zappalà et al. 2002). The difference is that NEO families will have a much faster dynamical evolution such that they are detectable over much shorter timescales as they diffuse into the orbital element space of the background objects. They also sample a much different range of parent asteroid sizes since the known sample of NEOs are much smaller than the known sample of MB objects.

The time scale of catastrophic collisions between MB asteroids that create asteroid families is short compared to the age of the Solar System. In catastrophic collisions, the colliding bodies completely shatter into smaller fragments, some of which are dispersed and then re-accumulate into objects on independent but similar orbits (Davis et al. 2002). The first groups of asteroids with nearly the same orbital elements were discovered by Hirayama (1918) and these groups are now known as *Hirayama families*. The members of each family

usually share similar spectral properties (Cellino et al. 2002), further suggesting a common origin in a single parent body that has undergone a catastrophic collision. We consider the members of this kind of asteroid family “genetically” related since they share the same parent body. At this time, more than 50 significant families have been tabulated in the MB (*e.g.*, Nesvorný et al. 2005).

MB families are identified by searching for enhancements in the space of *proper* orbital elements (a_p, e_p, i_p). A precise definition of the proper elements (*e.g.*, Knežević et al. 2002) is beyond the scope of this paper but it is sufficient here to think of them as long-term average orbital elements. This method is not readily applicable to NEOs for two main reasons: (1) the calculation of proper elements for NEOs is problematic due to the extremely chaotic evolution of NEO orbits and, (2) the limited population (3,319 objects as of 2005 Apr. 28) of known NEOs are spread over a much larger orbital element space than MB asteroids. Therefore, while asteroid families have long been recognized in the MB, the situation remains unclear regarding the existence of genetically related families other than meteor streams in the NEO population.

We have identified five possible mechanisms for the production of genetic NEO families:

1. NEO-MB asteroid collisions,
2. tidal disruption of NEOs,
3. intra-NEO collisions,
4. a MB family producing event near a MB resonance followed by rapid dynamical evolution of some of the members into NEO orbits, and

5. spontaneous NEO disruption.

Among the five, we consider the first two to be the most likely method for producing NEO families. Collisions between NEOs are expected to be rare (Bottke et al. 1996) since the density of NEOs interior to the MB is miniscule compared to the density of asteroids in the MB. The fourth mechanism is unlikely because there is only a small fraction of MB orbital element space near resonances capable of transporting the residue onto NEO orbits. Furthermore, the chaotic dynamical evolution during the transportation of the fragments to near-Earth orbits makes it unlikely that such a family could be identified as such based on their osculating elements. The last mechanism is reserved for objects with high volatile content, presumably comets that have worked their way into NEO orbits, and is probably the way meteor streams (e.g., Drummond 1981) are created. Thus, meteor streams are genetic NEO families but the members are orders of magnitude smaller than the smallest detectable NEOs.

The number of catastrophic NEO collisions per year that may produce families due to collisions on targets up to absolute magnitude H_{max} is given by:

$$N_{family}(< H_{max}) = \int_{-\infty}^{H_{max}} n(H) p_C(H) dH \quad (1)$$

where $n(H)$ is the differential number distribution of NEOs, and $p_C(H)$ is the annual probability of catastrophic collision, both given as a function of absolute magnitude. Using the NEO size-frequency distribution (SFD) of Bottke et al. (2002a) and the collision probability for MB asteroids from Fig. 14 of Bottke et al. (2005), we estimate that during the typical 10^6 year dynamical lifetime of NEOs (Morbidelli et al. 2002; Gladman et al. 1997) $\ll 1/8 \sim 1000$ NEOs larger than 10/1/0.1 km diameter are catastrophically disrupted. However, the catastrophic collision probability for NEOs is dramatically smaller than that of MB asteroids due to their much lower space-density (Bottke et al. 1996). Once an NEO is dynamically decoupled from the MB the collision probability drops even further. Thus, we consider it unlikely that any NEOs > 1 km diameter have suffered a family-producing event while the number of NEOs > 100 m diameter that have produced families is small.

An asteroid family produced in the disruption of a target would produce a large number of smaller asteroids. The SFD of the re-accumulated fragments may be determined through numerical modelling (e.g., Michel et al. 2002; Durda et al. 2005) or through studies of the SFD of known MB asteroid families (e.g., Tanga et al. 1999). The SFDs of the families are usually described by a power-law in the diameter D , $N(> D) \propto D^{-p}$, where $2 \lesssim p \lesssim 5$ for real MB families (e.g., Eunomia, Flora & Koronis) though it appears (Morbidelli et al. 2003) that the SFD of observed families becomes shallower for $H > 15$ ($D \lesssim 5$ km). The SFD of simulated new asteroid families displays a rich morphology (Michel et al. 2002; Durda et al. 2005) with a wide range of slopes that is difficult to characterize with a single power-law over the entire range of sizes but they are qualitatively similar to the observed SFD.

For the purpose of quickly estimating the expected number of known fragments due to a NEO family producing event, we assume that the fragments have a SFD similar to the known families with $2 \lesssim p \lesssim 5$. In a barely catastrophic collision the largest fragment (LF) has half the mass of the target. Since we know that $M \propto V \propto D^3$ and that the diameter of an

asteroid is related to its absolute magnitude by $D \propto 10^{-H/5}$, then it is simple to show that $H_{LF} = H_T + 0.5$ where H_T is the absolute magnitude of the target. By definition, $N(\leq H_{LF}) = 1$, and thus $N(\leq H) = 10^{\alpha(H-H_T-0.5)}$ so that the differential HFD for the fragments must be:

$$n(H) \sim 2.3 \alpha 10^{\alpha(H-H_T-0.5)} \quad (2)$$

with $0.4 \lesssim \alpha \lesssim 1.0$ and H_T being the absolute magnitude of the target.

If the actual and known population in a volume $dadedidH$ are represented by dN and dn respectively, then $dn = \epsilon(a, e, i, H) dN$ where ϵ is the observational completion of NEOs with orbital elements in the range $a \rightarrow a + da$, $e \rightarrow e + de$, $i \rightarrow i + di$ and $H \rightarrow H + dH$. The number of known fragments from the collision is then

$$N_{known} = \int_{-\infty}^{+\infty} n(H) \epsilon(H) dH \quad (3)$$

where $\epsilon(H) \sim \epsilon(a', e', i', H)$ and (a', e', i') are the mean orbital elements corresponding to a particular family.

Using reasonable estimates for $\epsilon(H)$ and the full range of possible slopes for the SFD, we find that the number of detectable fragments in a NEO family produced in the collision with a 1 km diameter target varies from essentially zero to many tens of thousands (if the family has the most steep SFD). This has tremendous implications for the formation of hazardous NEO families and spikes in the collision probability with the Earth. However, as argued above, the catastrophic disruption of a 1 km diameter NEO is highly unlikely. In the case of a 100m diameter NEO target the number of observable fragments is essentially zero. The fragments would be very small and would quickly begin to evolve apart dynamically and be strongly affected by non-gravitational forces (e.g., Yarkovsky forces: see Bottke et al. 2002b, for a review). Our ability to recognize a genetically related NEO family will depend on the efficiency of the employed algorithm and the time scale for decoherence of the members' orbits. We will explore both these factors in this work.

Thus, it would seem unlikely that observable NEO families can be produced and identified in the known NEO population. That being said, the opportunity of finding an NEO family would be important to asteroid physical studies and would also allow us to refine our understanding of the catastrophic disruption process and statistics. In a similar vein, Pauls and Gladman (2005) have studied the decoherence of "meteorite streams" to determine if time-correlated meteorite falls exist.

Drummond (1991, 2000) made the first attempts at searching for groupings in the known NEO population. His study was based on a D -criterion analysis (orbit similarity) of *osculating* orbital elements. Osculating elements are the instantaneous 2-body (Sun+object) orbital elements for an object. He discovered 14 associations, 8 strings and 7 pairs out of a sample of 708 NEOs. Briefly, associations are density enhancements above the local background in a four-dimensional D -criterion space (the values in each of the four dimensions are functions of an object's five *osculating* elements not including the mean anomaly). Strings are sets of NEOs in which every member is "connected" to at least one other member with D -criterion less than a specified threshold value, and pairs are two objects that have orbits that are statistically determined to be improbably close. These groupings contain a total of 155 NEOs or $\sim 22\%$ of the entire sample known at the time of Drummond's study.

At this time, 56 objects in his groupings (36%) have been taxonomically classified¹ but there is no obvious correlation between the taxonomic types in his groupings. Moreover, there are cases where very different taxonomic types exist within the same grouping — for instance, both S-type and F-type NEOs exist in the A1 association (the largest association identified by Drummond (2000), see Table 1). In MB families there is a high degree of correlation between the colors or taxonomic types of objects associated with each family (e.g., Nesvorný et al. 2005; Cellino et al. 2002). The fact that there exists heterogeneity in Drummond’s (2000) NEO associations may be used to argue that the groups are not genetically related families. Alternatively, it may be argued that the groups represent the fragments of an inhomogeneous parent body. The latter explanation is probably unlikely given that the NEOs are themselves probably fragments from collisions that took place within the MB.

In this paper we test the significance of the purported NEO families through various numerical simulations. First, we briefly describe (§2) the analysis technique employed by Drummond (1991, 2000). In §3 we discuss the statistical significance of the detections by attempting to search for groupings in synthetic NEO populations where no genetic families exist. We then demonstrate the decoherence of synthetic A1-like families as they evolve under only the effect of gravitational forces in §4 and study the dynamical evolution of the actual A1 association in §5. These studies allowed us to develop a technique for identifying real families within the NEO population as described in §6. We discuss our main results in §7 and close with a summary in §8.

2. NEO FAMILY IDENTIFICATION

Several versions of the D -criterion have been introduced (e.g., Southworth and Hawkins 1963; Drummond 1981; Jopek 1993; Valsecchi et al. 1999) to quantify orbital similarities. The dimensionless D -criterion used in Drummond (2000) and adopted in this study was defined by Southworth and Hawkins (1963) as:

$$D = \sqrt{d_1^2 + d_2^2 + d_3^2 + d_4^2}, \quad (4)$$

where

$$d_1^2 = \left(\frac{q_1 - q_2}{AU}\right)^2; \quad d_2^2 = (e_1 - e_2)^2; \\ d_3^2 = [2 \sin(I/2)]^2; \quad d_4^2 = [(e_1 + e_2) \sin(\Pi/2)]^2 \quad (5)$$

and

$$I = \arccos[\cos i_1 \cos i_2 + \sin i_1 \sin i_2 \cos(\Omega_1 - \Omega_2)] \quad (6)$$

$$\Pi = \omega_1 - \omega_2 + 2 \arcsin\left[\cos \frac{i_1 + i_2}{2} \sin \frac{\Omega_1 - \Omega_2}{2} \sec \frac{I}{2}\right]. \quad (7)$$

The subscripts 1 and 2 refer to the two orbits being compared, and the sign of the arcsin term of Eq. 7 changes when $|\Omega_1 - \Omega_2| > 180^\circ$. $q = a(1 - e)$ is the perihelion distance, e the eccentricity, i the inclination, ω the argument of perihelion, and Ω the longitude of the ascending node.

The D -criterion is a dimensionless distance metric in a four-dimensional space. The volume search method introduced by Drummond (2000) to identify associations searches for density enhancements above the local background around every object in the sample in this four-dimensional space. It

estimates the local background level by fitting a uniform local background and a Gaussian association (a gamma distribution) simultaneously to the cumulative distribution of D^2 around each orbit², and a candidate group is identified if the association plus background model gives a better fit to the data than the background-only model. Those asteroids with D -criterion less than the value at which the association density equals the background density are gathered to form a mean orbit around which the cumulative distribution of D^2 is fit for the two models again. The procedure iterates until it converges on a stable group of objects. The groupings detected in this way were termed *associations* by Drummond (2000).

We also searched for *pairs* and *strings* based on the D -criterion in a manner similar to that employed by Drummond (2000). A couple of NEOs are a pair if the D -criterion between the two is below a cutoff D_{pair} . Similarly, a string of NEOs is a set of objects in which every member is connected to at least one other with a $D < D_{string}$. In Drummond (2000), a cutoff of $D_{string} = 0.115$ was chosen under the guidance of the results from the volume search. We set a more stringent threshold, $D_{string} = D_{pair} = 0.1$, throughout this paper for the reason discussed below (§6).

In Drummond’s (2000) study, the search for groupings was performed on a sample of 708 NEOs (through 1999 HF1) listed on the Minor Planet Center (MPC) homepage as of 1999 April 22. As a test of our code, we attempted to reproduce Drummond’s associations by running our volume search code on the same sample. Like Drummond (2000) we often identified overlapping associations in which one association was partially or wholly contained within another. We eliminated the *smaller* of any two associations that shared more than 66% of its members with the larger group. Fig. 1 shows that our result is slightly different from Drummond (2000) although there is rough agreement in the distribution of the sizes of the associations. Table 2 compares the sizes and overlap between the four largest associations found in this work and in Drummond (2000). There is clearly a great deal of overlap between the groupings found in both works but the relationship is not perfect.

We believe there are three main reasons for the disagreement: (1) The orbital elements for the 708 NEOs are no longer identical to what they were five years ago. Most of these objects have much better orbits now due to new observations provided to the MPC in the intervening time period; (2) The volume search technique is very sensitive to the input orbital elements. Convergence of the iterative technique for identifying associations can alter membership by a few objects with changes in the D -criterion of only 0.01 (If all the difference between two orbits is in either a or e then $\Delta a = 0.01$ or $\Delta e = 0.01$ respectively). Reproducing the osculating elements of the 708 NEOs used by Drummond would be a monumental task involving extracting only those detections known to be associated with each object at the time that Drummond (2000) obtained the orbital element data and then determining the orbit; (3) The technique often identified overlapping associations that shared many members. As described above, when the overlap between two groups exceeded 66% the smaller one was discarded which biases our method towards larger groups.

Since we believe that our technique is demonstrably identi-

¹ Data collected from the PDS Asteroid/Dust Subnode, <http://www.psi.edu/astsubnode.html>

² We used *Pikaia* 1.2 (Charbonneau 2002), a FORTRAN version of a genetic search algorithm, as our non-linear least square fitting code to find the global minimum χ^2 .

cal to Drummond (2000) given the result shown in Fig. 1 we proceed with the use of the contemporary osculating elements for all 708 NEOs.

3. STATISTICAL SIGNIFICANCE OF NEO GROUPS

Drummond (2000) tested his NEO grouping software on synthetic populations of NEOs but did not, apparently, take into account observational selection effects when creating those populations. This is not surprising considering the difficulties involved in creating a realistic NEO population and then simulating the surveying capability of the many observatory programs that contributed to the 708 NEOs in his sample. Drummond tested the veracity of his groupings by performing the volume search on two sets of randomized orbital elements and comparing them to the results for the real set. He concluded that 50 to 70% of the groupings he had found might not be real.

Since that time, a good four-dimensional orbital element and absolute magnitude model of the NEOs has been developed by Bottke et al. (2002a) and good matches have been obtained between simulated NEO surveys and the known objects (*e.g.*, Raymond et al. 2004; Jedicke et al. 2003).

To test the statistical significance of the NEO groups that we identified (see Fig. 1), we generated 100 separate synthetic NEO models according to the (a, e, i, H) distribution of Bottke et al. (2002a). Each of the three angular elements of the orbits were generated randomly in the range $[0, 2\pi)$. We then passed each of them through a survey simulation similar to those of Jedicke et al. (2003) until the simulated survey detected 708 NEOs, identical to the size of the NEO sample used in Drummond’s (2000) analysis. Very briefly, the simulator attempts to mimic the average surveying capability of all surveys that have identified NEOs. It covers a 180° wide range in RA and from -30° to $+80^\circ$ in declination in the space of 14 days centered on new moon each lunation. We found that using a limiting magnitude of $V = 20.5$ (50% efficiency) where the efficiency drops from 100% to 0% in the range from $V = 19.75$ to $V = 21.25$, and a minimum rate of motion to distinguish NEOs of $0.3^\circ/\text{day}$, yielded results that qualitatively agree with the observed distributions. The minimum and maximum range of the distributions of the 100 synthetic populations is shown in Fig. 2, in which it is clear that our simulation nicely bounds the observed distribution of NEO orbital elements and absolute magnitudes as utilized by Drummond (2000).

We used the volume search method to identify associations in our 100 synthetic NEO populations. In Fig. 3 we show the size distribution of all the associations detected in our synthetic NEO populations and the distribution of associations found (by our code) in the same NEO sample as used in Drummond (2000). Since no genetic families exist in the artificially generated NEO populations, the fact that we identified associations containing more than 20 members in that data, and that the size distribution of the groupings for the real data is similar to that for the synthetic data sets, brings into question the genetic nature of the associations reported by Drummond (2000).

Interestingly, both the synthetic and real data show a bi-modal distribution. When the size of the association is $\lesssim 15$ there is a power-law drop in the SFD. For associations containing $\gtrsim 15$ members the distribution is almost flat or modestly peaked near 22. We are unable to explain why the technique produces this bi-modal distribution. It is *not* the case that the synthetic model may contain synthetic genetic

families *because* the actual NEO population from which it was derived contains genetic families. This is a result of the technique used to generate the NEO model as detailed in Bottke et al. (2002a). Briefly, the correlation between the orbital elements of members in the actual NEO population was lost in the fitting procedure employed by Bottke et al. (2002a). When we generated our synthetic NEO population it therefore has no memory of any possible groupings in the real NEO population.

We test whether the real NEO population is more clustered than the synthetic ones by determining if the two populations are different or drawn from the same underlying distribution function. The Kolmogorov-Smirnov (K-S) test (*e.g.*, von Mises 1964; Kolmogorov 1933; Smirnov 1933) is one of the most generally accepted techniques for testing the consistency of two one-dimensional distributions. It is applicable to non-gaussian distributions and works well on small sample sizes. We applied the K-S test to compare the size distribution of the associations found in the real NEO population and that found in each of the 100 synthetic NEO populations. We found that the size distributions of the associations detected in 35 (54) out of the 100 synthetic populations are consistent with that of the associations detected in the real NEO population at a significance level $\geq 95\%$ (85%). Figure 4 shows the cumulative distribution of the K-S probability that the synthetic data sets are consistent with the actual data. Thus, there appears to be little reason to believe that any of the associations detected by Drummond (2000) in the actual NEO sample are real.

4. DECOHERENCE OF A SYNTHETIC A1-LIKE FAMILY

In this section we determine the length of time that a synthetic genetic NEO family like Drummond’s (2000) A1 association would be detectable using the D -criterion technique. This is important for understanding whether the A1 association is real and also for calculating the expected number of NEO families that may be detectable in the future.

A significant fraction of the A1 association’s mean orbit overlaps the MB so we assume that, if it is real, it was most likely created in a collision between a NEO and a MB asteroid as opposed to one of the other four possible mechanisms identified in §1. Current computing techniques allow a realistic simulation of the entire process of the formation and evolution of asteroid families within a reasonable amount of clock time (*e.g.*, Michel et al. 2002; Durda et al. 2004). We have performed a smooth-particle hydrodynamics (SPH) simulation (as in Durda et al. 2004) of a NEO-MB asteroid collision from which an A1-like family was formed, tracked the re-accumulation process, and then followed the dynamical evolution of the individual fragments. It should be noted that some recent works (*e.g.*, dell’Oro et al. 2004; Cellino et al. 2004) suggest that detailed SPH models may underestimate the ejection velocities amongst the collision fragments.

First, we specify the parent body for the collision: assuming that the A1 association is a genetic family we set the orbit of the synthetic A1 parent body to the mean orbit of the actual 25 A1 members, *i.e.*, $(a, e, i, \Omega, \omega) = (2.21 \text{ AU}, 0.49, 4.1^\circ, 194.3^\circ, 123.3^\circ)$.

The lower limit on the size of the parent body is the sum of the volume of the 25 A1 members which is dominated by the largest fragment, 1627 Ivar. Veeder et al. (1989) reported radiometric observations of this object and 2368 Beltrovata (the third largest member of A1) and Delbo et al. (2003) provide independent radiometric observations of 1627 Ivar. De-

pending on the thermal model used, Veeder et al. (1989) determined a visual geometric albedo of 0.08 or 0.12 to 1627 Ivar and 0.05 or 0.13 to 2368 Beltrovata. Delbo et al. (2003) found a visual geometric albedo for 1627 Ivar of 0.20, 0.15, or 0.050 depending on whether the STM, NEATM, or FRM thermal model was used. On the other hand, the effective diameter for 1627 Ivar was estimated to be 8.5 ± 3 km from radar measurements (Ostro et al. 1990). Given the widely varying albedo estimates from radiometric observations and thermal modelling, we decided to use the radar measurements as the basis for our constraints on, and best estimate for, the diameter of the A1 parent body.

Table 1 shows the absolute magnitude (H), taxonomic type (where available), and effective diameter (lower bound, best estimate, upper bound) for each object in A1. The H values for each object are from the Lowell Observatory’s ASTORB database (<ftp://ftp.lowell.edu/pub/elgb/astorb.html>). The lower limit for the A1 parent body is shown for three different albedo values at the bottom of the table. Note that the albedo values ($p_V = 0.07 \rightarrow 0.306$) in this table encompass all of the albedo estimates from radiometric measurements ($0.07 \rightarrow 0.26$) for 1627 Ivar, hence we believe 9.8 ± 3.5 km is a suitable estimate for the size of the A1 precursor. For the purpose of our simulations we round this number to a synthetic A1 precursor diameter of 10 km.

We note that Tanga et al. (1999) claim that a better preliminary estimate of the parent body size based on geometrical considerations is obtained merely by summing the diameters of the first and third largest asteroids in the family. They state that this is a much better estimate of the parent body diameter when the volume method (as used in this analysis and described above) yields a diameter less than the sum of the two largest family members. Using their technique our best estimate for the diameter of the A1 association parent body would be about 12 km.

With the target asteroid specified we then determine the relevant properties of the impactor. We assumed that the orbital elements of the impactor are equal to those of a MB object that is likely to collide with the A1 precursor. We identified these orbital elements in the following manner. The MB asteroids are almost complete to $H \sim 14.5$, so we made a histogram of the semi-major axis of all MB objects with $H < 14.5$ that could hit the A1 precursor. Since the A1 precursor’s heliocentric distance ranges from perihelion at ~ 1.1 AU to aphelion at ~ 3.3 AU, we examined all MB semi-major axes with $1.1 \text{ AU} < a(1 - e) < 3.3 \text{ AU}$ and found that the most probable semi-major axis for the projectile is ~ 3.1 AU. Similarly, the most probable eccentricity is ~ 0.11 and inclination is $\sim 10.0^\circ$. Therefore, we select as our impactor an object with $(a, e, i) = (3.1 \text{ AU}, 0.11, 10.0^\circ)$.

We assume that the collision takes place at a speed equal to the most probable collision speed for an object with A1’s mean orbit — 8.36 km/s (Bottke 2003, personal communication).

The most likely location of an impact event is near the aphelion of the A1 precursor since it spends most of its time near that heliocentric distance. The range of overlapping heliocentric distances between the orbits of the A1 precursor and the projectile is from 2.94 AU to 3.30 AU, but the actual range where the impact could happen is more restricted because we have fixed the impact speed. At higher heliocentric distances (> 3.09 AU) the relative impact speed dictates that the relative inclination (the angle between the planes of the two orbits) must be larger than the highest possible inclination difference,

which is the sum of the two inclinations (14.1°). The loop in Fig. 5 shows the relationship between the relative inclination and the heliocentric distance of the impact when constrained by our choice of the impact speed. The dashed lines in the figure bound the region of permitted relative inclinations between the A1 precursor and the projectile, *i.e.*, smaller than $i_1 + i_2$ and larger than $|i_1 - i_2|$ where the subscripts 1 and 2 refer to the target and projectile. For our simulations we used the smallest and largest allowable heliocentric distances from Fig. 5 (2.94 AU and 3.09 AU) and the one at which the relative inclination is the smallest (2.98 AU) in order to investigate the dependence of the decoherence time scale upon the impact location.

Since we require that the collision occurs at a specific heliocentric distance and speed, the three angular orbital elements of the impactor can be determined because the location of the A1 precursor at the time of collision is known and the impactor has no choice but to cross the same point at the same time. We note that there are two solutions — the impactor may collide on either hemisphere relative to the velocity vectors of the two objects. We present the results for only one case since both give essentially identical results.

We modelled the initial stages of the impact with the 3-dimensional SPH code SPH3D (Benz and Asphaug 1995). In keeping with our pattern of favoring the most probable event, we selected the smallest possible impacting object that would produce a barely catastrophic disruption. Based on our previous experience with impact simulations, and scaling the values for the velocity of the impact and size of the target, we selected an impactor of 0.25 km diameter. We will argue later that this is probably too *large* an impactor but we believe that the results of the simulation are still of practical utility. Similarly, the most probable impact angle is 45° as used in this simulation.

The 10 km diameter target was comprised of 100,000 SPH particles and, to roughly match the SPH particle volume density of the target, the impactor is comprised of 700 particles. In this simulation the A1 precursor was catastrophically disrupted and shattered into thousands of independent fragments by the impactor. The SPH phase of the simulation followed the impact for 100 seconds after which time the ejecta flow fields were well established and no further fragmentation or damage was observed.

The outcome of the SPH simulation was handed off as the initial conditions for an N-body simulation using the cosmologically derived pkdgrav code (Richardson et al. 2000; Leinhardt et al. 2000; Leinhardt and Richardson 2002) that followed the trajectories of the ejecta fragments for sufficient time to allow gravitational re-accumulation of the larger collision fragments. This technique was used by Durda et al. (2004) to model the formation of asteroid satellites resulting from large impacts on 100-km scale MB asteroids. With the small sized target assumed here for the A1 precursor, there is not much gravitational re-accumulation among the largest fragments and the N-body phase of the simulation need only be run for 200 N-body timesteps (each step corresponding to about 50 s) in order to establish fragment positions and ejection velocities.

From the velocity vectors of the A1 precursor and the impactor at the collision location we can derive the three Euler angles between the impact space, where the simulation was performed, and the external heliocentric orbital space in which we follow the post-collision dynamical evolution of the fragments. The initial orbits of the re-accumulated frag-

ments are handed over to Mercury6 (Chambers 1999) to follow their dynamical evolution. The SPH simulation produced 1243 fragments down to a diameter of 216 m (pre-determined by the resolution of the simulation). Note that the smallest diameter amongst known members of the real A1 association is only 130 ± 50 m (see Table 1).

Only a fraction of the fragments would be discovered in reality, so we applied an *ad hoc* observational selection function to determine which of the synthetic fragments were detected. The correction factor is a complicated function of a survey’s performance characteristics and the orbital element distribution of the detected objects (Jedicke et al. 2002). Since all the synthetic A1 family members have essentially identical orbital elements we would like to determine the selection effect as a function of H for all the surveys that contributed to finding NEOs with orbital elements similar to the A1 mean orbit. This would be difficult if not impossible to determine in practice. Instead, we chose simply to divide the set of all known 708 NEOs at the time of Drummond’s (2000) analysis as a function of absolute magnitude, $n(H)$, by the debiased “true” distribution of NEOs according to Bottke et al. (2002a). We fit the resulting distribution to a function of the form:

$$P(H) = \frac{1}{e^{\frac{H-L}{W}} + 1}, \quad (8)$$

and found $L = 15.82 \pm 0.19$, $W = 1.15 \pm 0.11$. $P(H)$ gives the probability that an NEO with absolute magnitude H would have been discovered by the time of Drummond’s (2000) analysis.

We applied this discovery probability with the central values for L and W to the re-accumulated synthetic A1 family. An albedo of 0.128 (the same as was used for the best estimate of the size of the A1 precursor as in Table 1) was used to convert the size of the objects into an absolute magnitude. Running many trials for this process (which objects “survive” the selection function of equation 8 is random) yielded a mean size of an observed synthetic A1 family of 25 ± 4 members compared to the 25 members of the actual A1 association reported by Drummond (2000). The size distribution of our synthetic population is compared to the actual size distribution in Fig. 6.

It appears that our model does not reproduce the actual A1 association’s size distribution. This could be due to our having selected an impactor that caused far too much damage to the target, shattering it with such violence that the fragments were unable to gravitationally accumulate into larger objects. However, considering that our dynamical integrations of the fragments consider only gravitational effects, the SFD of the fragments is probably not important to the remainder of this study.

We now examine the decoherence of the synthetic A1 family as its members dynamically evolve under the gravitational influence of the Sun and eight planets (Mercury through Neptune). It was only necessary to integrate the motion of the 25 fragments that were detected rather than the ensemble of 1242 fragments. The orbits were propagated forward in time using a hybrid symplectic/Bulirsch-Stoer integrator (Mercury6, Chambers 1999) with a step-size, τ , of 30 days (*i.e.*, 1/40 of the shortest initial orbital period amongst the fragments). We verified the result by comparing it to an identical run on the same fragments using the general Bulirsch-Stoer integrator with the same step-size.

In reality, this evolution occurs within a population of background objects that are also interacting gravitationally with

the major objects in the solar system and with each other. In order to save time, for the purpose of this study, we decided not to integrate the motion of all the background objects. Instead, we used two different static background NEO populations: B1 was a randomly selected synthetic NEO population (from §3) with 708 objects and B2 was formed using the same 708 NEOs as used in Drummond’s study but removing the 25 actual A1 members. This means that our static background populations possessed a slightly different mean density in orbital element space with a total of $733=708+25$ objects in the B1 case and only 708 objects in the B2 case. This introduces a difference in the mean density of only a few percent. It would be difficult to correct because it would require selectively removing 25 members from the synthetic B1 population that somehow match the original A1 members. Instead, we chose to ignore this small difference in density and note that, in any event, it makes the identification of groupings in the synthetic B1 data slightly more likely. We introduced our synthetic A1 family members into the background NEO populations and search for groupings every 2,000 years as the A1 family evolves in time. Since our purpose was to track the evolution of the A1 family, we only performed the volume search for candidate groupings around the 25 detected fragments as opposed to searching the entire sample. The mean orbit of the resulting association may be beyond the boundary of the original fragments because interloping asteroids may be incorporated into the final association due to the iterative aspect of the volume search technique.

While our definition of associations, strings and pairs matches that of Drummond (2000) our manner of selecting the final groups may be different. We searched for associations using the (known) synthetic A1 members as seeds and select the association that includes the most members of the original synthetic family. If multiple associations meet this criteria then we selected the association containing the smallest number of interlopers. Similarly, strings were identified using the synthetic A1 members as seeds and selecting the string that contains the most members of the original association. Once again, if multiple strings met this criterion we used only the string that contained the least interlopers. Finally, pairs were identified only for objects within the original synthetic A1 association in the current timestep.

Fig. 7 demonstrates the decoherence of an A1-like family from creation until it is 1 Myr old. The results for other choices of the 25 detected fragments, the NEO background and for the heliocentric distance of impact appear nearly identical. It shows that the rapid orbit evolution of NEOs mixes the genetically related synthetic A1 objects and background objects within ~ 300 Kyr so that the association becomes undetectable to this technique. The fact that all our runs have similar results indicates that the decoherence time scale is independent of the choice of the background NEO population and the location where the precursor is disrupted.

5. DECOHERENCE OF THE ACTUAL A1 ASSOCIATION

The A1 association is the largest among the 14 identified by Drummond (2000) and all its 25 members are included in the largest association identified in this study (see Table 2). It is the most statistically significant association found using our technique and the 25 common members have a mean orbit of $(a, e, i) \sim (2.21 \text{ AU}, 0.49, 4.1^\circ)$. In §4 we argued that the A1 association must have derived from a parent body $\gtrsim 10$ km in diameter if it represents a genetic NEO family, yet we calculated in §1 that the production of a family from the dis-

ruption of an object this large is extremely unlikely. However, just because an event is unlikely doesn't mean that it did not occur.

In this section we use two different methods to examine the possibility that Drummond's (2000) A1 association is a bona fide genetic family or due merely to chance alignments or observational biases. First, we integrate forward the orbits of all the A1 members and see how long it remains detectable as an association. If the association is real we would expect that the members remain an association for some time into the future. Second, we integrate the orbits *backward* in time to see if their angular orbital elements converge, indicating a common point of origin at some time in the past. The backward integration is justified for this association because we know that, if it is a genetic family, it can not be very old. The latter technique has been used by Nesvorný et al. (2002) to determine the age of the Karin cluster within the MB.

The orbits of the 25 members in A1 were propagated forward (and backward, §5.1) in time using the general Bulirsch-Stoer integrator with $\tau = 20$ days (*i.e.*, 1/40 of the shortest initial orbit period amongst the actual A1 members). The current orbital elements of the A1 members are extracted from the MPCORB database as of 2005 March 1 (<ftp://cfa-ftp.harvard.edu/pub/MPCORB/>) that contains accurate orbital elements derived from multi-opposition observations of the NEOs. Once again, the integration took into account the gravitational perturbations due to all major planets (Mercury through Neptune) but neglected the evolution of background NEOs. Every 2,000 years we searched for groupings (pairs, strings & associations) in the same sample as used by Drummond (2000) using the techniques described above but replacing the 25 A1 members with their evolved orbits.

For the same reasons as in §4, we only searched for density enhancements above the local background using the 25 A1 members as seeds in the volume search. We searched for strings and pairs within the A1 association at each time step in a manner identical to that described in §4.

Fig. 8 shows the evolution of A1 during the next 500 Kyr. The A1 members rapidly evolve away from each other as shown in Fig. 8A — the average D -criterion amongst all A1 members increases from 0.2 to >0.6 in ~ 20 Kyr and to nearly 1.0 after slightly more than 200 Kyr. At the first time step (*i.e.*, now), all the 25 A1 members are included in our 29-member association (Fig. 8B), but after just two time steps (4,000 years) the association is essentially undetectable. In the following 500 Kyr the largest A1-like associations contain anywhere from a few to about 30 objects but those groups contain only a few of the original A1 members. In other words, those associations are quickly and heavily contaminated by interlopers.

The situation is similarly bleak for strings (Fig. 8C) and pairs (Fig. 8D) detected within the associations at each time step. The largest string detected at the first timestep contains only 5 members and after just 20,000 years not a single time step ever contains more than 4 members of the original A1 cast. Similar behavior is observed for the pair counts within the original A1 members. With 25 objects there are 300 possible unique pairings but the maximum number of pairs within the A1 association is 10 for only the very first time step.

The result that the A1 association is essentially undetectable within ~ 10 Kyr suggests that it too is merely a statistical fluctuation in the density of NEO orbital elements and argues against the genetic nature of A1. It is extremely unlikely that such a large association would be detected just as

this technique lost its ability to identify it due to the orbital decoherence of its members.

5.1. Evolution of the A1 association's Ω and ω

Nesvorný et al. (2002) integrated the orbits of members of the Karin cluster backwards in time to identify when the longitude of ascending node (Ω) and argument of perihelion (ω) of all members were tightly clustered. These angular orbital elements evolve rapidly and secularly under the influence of the gravitational perturbations of the planets. Determining the point in time at which the values were tightly clustered allowed them to accurately date the age of that small and new asteroid family. The evolution of these angular elements will be considerably faster for NEOs but we tested for their convergence despite the low probability of success.

Figure 9 shows the evolution of the node and perihelion angles for the last 50 Kyr. We only show the evolution over this reduced time period because it is representative of the entire evolutionary period of this association (see next paragraph for discussion). Note that at $t = 0$ the values are not consistent with being randomly distributed since the D -criterion technique specifically selects sets of objects with non-random orbits (in Ω and ω as well as a , e and i). All 25 values of the longitude of ascending node are distributed in the restricted range $125^\circ \lesssim \Omega \lesssim 325^\circ$ and while the longitude of perihelion is similarly restricted in the range $0^\circ \lesssim \omega \lesssim 180^\circ$.

To evaluate whether these orbital elements become less random in the past, in other words, more “clumped”, we determined the probability that the elements were consistent with being flatly distributed using the K-S test at each time step. This test was uninformative, the distribution changing rapidly and randomly from consistent to inconsistent over the entire 300 Kyr period. The problem is that there are many ways for a distribution to be “clumped”. Instead, we resorted to examining the distribution of Ω and ω in terms of their range, and RMS spread within that range, as a function of time as shown in Fig. 10. The range of the two elements and their RMS spread within that range is at a minimum at the present time. In other words, at no time in the past were these angular elements more “clumped” than at the present time. The “clumpiness” at the present time is easily explained as a consequence of the D -criterion technique selecting clumps in their orbit distribution. Once again, this result contradicts the hypothesis that the A1 association represents a genetically linked set of asteroids.

6. IDENTIFYING ACTUAL GENETIC FAMILIES

The fact that the volume search method identified a number of “associations” in synthetic NEO populations where no genetic families exist (§3) indicates that the method, by itself, can not distinguish between genetic families and random, over-dense regions in the orbit element space. In this section we show that, in principle, it should be possible to separate the real genetic families from the background by combining results from the volume search and string/pair searches.

In §4 we showed that a genetic NEO family loses D -criterion coherence ~ 250 Kyr after creation. However, even after the family diffuses into the background the volume search method still detects associations with > 15 objects (Fig. 7B) but most of the members of these associations are interlopers from the background. The question is then how to distinguish between associations containing actual genetically related members and those containing interlopers.

Comparing Fig. 7B with Figs. 7C&D reveals a clear difference between the evolution of the association size and the string size *or* total number of identified pairs — after the family loses coherence the association size becomes very noisy, jumping erratically between small and large families; while the string size and number of pairs drops to a near steady-state value with little variation from time step to time step. We utilize the difference in behaviour between associations, strings and pairs to differentiate between real and false genetic NEO families in Fig. 11. In this simulation the strings are found using the members of the association identified at each time step as seeds. The pairs are identified only amongst the members of the association at each time step and the average D -criterion is also calculated only amongst the same members. Our intent is to mimic the fact that when searching for new genetic NEO families the members of the association will not be known *a priori* as in Figs. 7 and 8. In that figure the *pair fraction* is the total number of pairs identified within the association divided by $C_n^2 = n(n-1)/2$, the total number of possible unique pairs within the association when n is the number of objects it contains. The average D -criterion value is the sum of the D -criterion values between each unique pair of objects in the association also divided by C_n^2 . These two parameters essentially measure the “tightness” of an association. We expect that fresh genetic NEO families will be very “tight” with pair fractions approaching unity and average D -criterion value approaching zero. There is a very strong correlation between the pair fraction and average D -criterion value.

The data in Fig. 11 are for the synthetic A1 family of §4. Each data point represents a single time step in the dynamical evolution of the synthetic A1 family with the different symbols representing time since its formation. There is clearly a strong time-dependent evolution that may be used to differentiate between real and false genetic NEO families. The 0.1 D_{cutoff} is found empirically to yield the clearest separation between associations detected at different epochs. The black crosses in the figure represent the results of the same analysis applied to our synthetic NEO background populations (see §3). The groupings found in those populations (with no families) overlap with the ones found after the decoherence of the synthetic A1 family but are well-separated from the groupings found before the decoherence time of 250 Kyr. The current location of Drummond’s (2000) A1 association is indicated in Fig. 11 with a red star, and the other associations (A2 – A14) are marked with blue triangles.

7. DISCUSSION

We believe that the results described above bring into serious question the reality of any of the NEO associations reported by Drummond (2000). It is unlikely that a large NEO, similar in size to the precursor to Drummond’s (2000) A1 association, would have disrupted during the last 300 Kyr, the time frame during which the family of asteroids would be detectable with the D -criterion orbital similarity technique. The fact that the largest, and presumably most likely, association reported by Drummond (2000) would be unidentifiable in just a few hundred thousand years implies that, if it is real, it was found just in the ~ 250 Kyr period before the association becomes totally decoherent (see Figure 7). This represents a mere $\sim 10\%$ of the dynamical lifetime of typical NEOs and is in agreement with the decoherence time scales for NEO meteorite streams as reported by Pauls and Gladman (2005). Furthermore, the SFD of associations detected in the actual NEO sample matches the same distribution for associations

detected in a random sample of NEOs that accounts for observational selection effects.

Confusing the issue slightly, we applied our technique to all of Drummond’s (2000) original associations but using his more relaxed (D_{cutoff}) threshold on the D -criterion of 0.115 instead of our value of 0.1. All but one of these associations remained firmly in the region of random background fluctuations shown in Fig. 11. Only when using the original members of the A14 association as seeds with the relaxed D -criterion threshold did we detect a 5-member string (as opposed to a 2-member “string” with $D_{cutoff} = 0.1$) containing all four original A14 members (String Size/Association Size = 1.2). At the same time, we found 3 pairs amongst the four A14 members (*i.e.*, Pair Fraction = 0.5) compared to only 1 pair when $D_{cutoff} = 0.1$. In this case, A14 would be located in the more interesting region of Fig. 11 where genetic families may be identified, well beyond the noise region defined by the fake detections within the synthetic NEO populations. This hints that A14 may be a *genetic* NEO family but since it has only 4 members, losing or gaining a single member in the string would cause a 25% difference in the ratio of the string size to association size. Furthermore, our diagnostic technique is based on the simulation of a 25 member A1-like family rather than a 4 member A14-like family so the comparison is not strictly applicable.

On the other hand, we show in Section 4 that a NEO family *can* maintain coherence in its orbital elements for $\gtrsim 200$ Kyr. So the D -criterion technique may be useful for identifying NEO families that must then undergo further study before being classified as real. The supplementary studies should include at least a statistical study of whether groups of the identified size are unlikely in a similarly sized synthetic data set that incorporates all the known observational selection effects.

Strong support for the veracity of a putative association found by the volume search method may be obtained from its location in diagnostic diagrams similar to Fig. 11. All the points with pair fraction $\gtrsim 0.2$ and string size / association size $\gtrsim 0.8$ correspond to positive detections of real genetic associations with very few interlopers. Alternatively, the figure may be considered as demonstrating the intrinsic limits of D -criterion based methods in identifying families – only the tightest families (*i.e.*, youngest ones) can be solidly detected. We note that the current location of Drummond’s (2000) A1 is solidly in the territory occupied by random fluctuations.

We understand that we have only examined in detail a single association identified by Drummond (2000). It is possible that parent-body NEOs in other orbits may be more likely to disrupt and form longer living, more easily identified NEO families. It is also possible that one of the other methods of producing an NEO family may produce longer lived or more easily identifiable families. The different production mechanisms may even show a difference in the distribution of the orbital elements of their members during the early stages of their separated evolution.

For instance, the tidal disruption process (*e.g.*, Richardson et al. 1998) seems capable of producing contact and close binary asteroids and also families of objects on very similar orbits (*e.g.*, Comet Shoemaker-Levy 9, Boss (1994); crater chains on the various planets and their satellites, Bottke et al. (1997)). The fragments from this production process may well be detectable as a family long after the planetary close approach that produces the chain of objects. We plan on studying this possibility in future simulations.

The dynamical simulations of both the actual and synthetic A1 families (§5 and §4) did not account for the Yarkovsky effect (see Bottke et al. 2002b, for a review) that is known to cause diffusion of orbital elements for small objects in the MB. The effect of this non-dynamical force will be correspondingly greater for NEOs due to their approaching much closer to the Sun. Even so, the expected drift rate for a 100 m diameter NEO with $a = 1$ AU, $i = 45^\circ$ and typical density, albedo and surface conductivity, is only $\sim 2 \times 10^{-4}$ AU in 10^5 years (Nesvorný, personal communication). Thus, the Yarkovsky effect operates far too slowly to contribute to the decoherence of NEO families.

It is clear that contemporary studies of genetic NEO families are hampered by the small number of known NEOs thus, larger and deeper surveys are needed. Pan-STARRS will be the next major survey to come online and will detect as many asteroids and comets in one lunation as are currently known. Pan-STARRS will revolutionize our understanding of NEOs — while 3,319 NEOs are known as of April 2004 there are hundreds of thousands of NEOs brighter than Pan-STARRS' expected limit of $R \sim 24$ mag. 10,000 new NEOs should be discovered in the first year of operations alone. By the end of the first year of Pan-STARRS operation, the completeness of NEOs of 1 km (100 m) in diameter will be boosted to at least 90% (20%) from the current 75% (5%), and after 10 years of operation Pan-STARRS will discover almost all of the NEOs larger than 1 km diameter and more than half of the NEOs bigger than 100 m diameter. With a good understanding of the observational selection effects in a single survey it should be possible to identify NEO families or determine that there are none and use this information to constrain the collision rate of NEOs.

8. CONCLUSION

We find it unlikely that any of the enhancements in orbital element space for the known NEO population are due to a genetic relationship between the member objects. The primary

motivation for this conclusion is the fact that synthetic data sets that incorporate realistic distributions of NEOs and observational selection effects show the same distribution of density enhancements as the actual population. We also base our conclusion on the fact that the current understanding of NEO collision rates makes it extremely unlikely that a large enough NEO could have disrupted recently enough to allow its fragments to maintain enough coherence to remain detectable by the D -criterion technique.

We have identified a new technique that will allow future searches for genetic families within the known NEO population. The method relies on the tight clustering in the D -criterion during the first couple hundred thousand years after the production of the family. Once an association is identified, it is searched for strings and pairs. If the number of found pairs is more than $\sim 20\%$ of the maximum possible number of pairs in the association *and* the ratio of the maximum string size to association size is $\gtrsim 0.8$, then the association is likely to be a real genetic family.

Upcoming improvements in NEO survey technology such as Pan-STARRS may provide a large enough sample of NEOs in a single, well-characterized survey, to allow identification of NEO families or set a limit on their number. This, in turn, will allow dynamicists to refine their models of the collisional evolution of the solar system.

9. ACKNOWLEDGEMENTS

Scotti's salary is supported by these grants to R. S. McMillan: NASA Planetary Astronomy NNG04GK48G, NASA Near-Earth Object Observations NAG5-13328, U. S. Air Force Office of Scientific Research F49620-03-10107, and The Paul G. Allen Charitable Foundation. We thank Josh Barnes, Alberto Cellino, Jack Drummond, Nader Haghipour, Robert S. McMillan and David Nesvorný for constructive suggestions during the preparation of this manuscript.

REFERENCES

- Benz, W., Asphaug, E. 1995. Simulations of brittle solids using smooth particle hydrodynamics. *Computer Physics Communications* 87, 253-265.
- Boss, A. P. 1994. Tidal disruption of Periodic Comet Shoemaker-Levy 9 and a constraint on its mean density. *Icarus* 107, 422-426.
- Bottke, W. F., Nolan, M. C., Melosh, H. J., Vickery, A. M., Greenberg, R. 1996. Origin of the Spacewatch Small Earth-Approaching Asteroids. *Icarus* 122, 406-427.
- Bottke, W. F., Richardson, D. C., and Love, S. G. 1997. NOTE: Can Tidal Disruption of Asteroids Make Crater Chains on the Earth and Moon?. *Icarus* 126, 470-474.
- Bottke, W. F., Morbidelli, A., Jedicke, R., Petit, J., Levison, H. F., Michel, P., Metcalfe, T. S. 2002a. Debiased Orbital and Absolute Magnitude Distribution of the Near-Earth Objects. *Icarus* 156, 399-433.
- Bottke, W. F., Vokrouhlický, D., Rubincam, D. P., and Brož, M. 2002b. The Effect of Yarkovsky Thermal Forces on the Dynamical Evolution of Asteroids and Meteoroids. *Asteroids III*, 395-408.
- Bottke, W. F., Durda, D. D., Nesvorný, D., Jedicke, R., Morbidelli, A., Vokrouhlický, D., Levison, H. F. 2005. Linking the Collisional History of the Main Asteroid Belt to its Dynamical Excitation and Depletion. in press.
- Cellino, A., Bus, S. J., Doressoundiram, A., and Lazzaro, D. 2002. Spectroscopic Properties of Asteroid Families. *Asteroids III*, 633-643.
- Cellino, A., dell'Oro, A., and Zappalà, V. 2004. Asteroid families: open problems. *Planet. Space Sci.* 52, 1075-1086.
- Chambers, J. E. 1999. A hybrid symplectic integrator that permits close encounters between massive bodies. *Monthly Notices of the Royal Astronomical Society* 304, 793-799.
- Charbonneau, Paul. 2002. An introduction to genetic algorithms for numerical optimization. NCAR Technical Note TN-450-IA.
- Davis, D. R., Durda, D. D., Marzari, F., Campo Bagatin, A., and Gil-Hutton, R. 2002. Collisional Evolution of Small-Body Populations. *Asteroids III*, 545-558.
- dell'Oro, A., Bigongiari, G., Paolicchi, P., and Cellino, A. 2004. Asteroid families: evidence of ageing of the proper elements. *Icarus* 169, 341-356.
- Delbo, M., A. W. Harris, R. P. Binzel, P. Pravec, and J. K. Davies. 2003. Keck observations of near-Earth asteroids in the thermal infrared. *Icarus* 166, 116-130.
- Durda, D. D., Bottke, W. F., Enke, B. L., Merline, W. J., Asphaug, E., Richardson, D. C., Leinhardt, Z. M. 2004. The formation of asteroid satellites in large impacts: results from numerical simulations. *Icarus* 170, 243-257.
- Durda, D. D., Bottke, W. F., Nesvorný, D., Asphaug, E., and Richardson, D. C. 2005. Size-frequency distributions of fragments from SPH/N-body simulations: Comparison with observed asteroid families. *Lunar Plan. Sci.* XXXVI, abstract no. 1876.
- Drummond, J. D. 1981. A test of comet and meteor shower associations. *Icarus* 45, 545-553.
- Drummond, J. D. 1991. Earth-approaching asteroid streams. *Icarus* 89, 14-25.
- Drummond, J. D. 2000. The D Discriminant and Near-Earth Asteroid Streams. *Icarus* 146, 453-475.
- Gladman, B. J., Migliorini, F., Morbidelli, A., Zappala, V., Michel, P., Cellino, A., Froeschle, C., Levison, H. F., Bailey, M., and Duncan, M. 1997. Dynamical lifetimes of objects injected into asteroid belt resonances. *Science* 277, 197-201.
- Hirayama, K. 1918. Groups of asteroids probably of common origin. *Astronomical Journal* 31, 185-188.
- Jedicke, R., Larsen, J., and Spahr, T. 2002. Observational Selection Effects in Asteroid Surveys. *Asteroids III*, 71-87.

- Jedicke, R., Morbidelli, A., Spahr, T., Petit, J., Bottke, W. F. 2003. Earth and space-based NEO survey simulations: prospects for achieving the spaceguard goal. *Icarus* 161, 17-33.
- Joepk, T. J. 1993. Remarks on the meteor orbital similarity D -criterion. *Icarus* 106, 603.
- Knežević, Z., Lemaître, A., and Milani, A. 2002. The Determination of Asteroid Proper Elements. *Asteroids III*, 603-612.
- Kolmogorov, A. N. 1933. Sulla determinazione empirica di una legge di distribuzione. *Giornale dell'Istituto Italiano degli Attuari*, 4, 83.
- Leinhardt, Z. M., Richardson, D. C. 2002. N-Body Simulations of Planetesimal Evolution: Effect of Varying Impactor Mass Ratio. *Icarus* 159, 306-313.
- Leinhardt, Z. M., Richardson, D. C., Quinn, T. 2000. Direct N-body Simulations of Rubble Pile Collisions. *Icarus* 146, 133-151.
- Michel, P., Tanga, P., Benz, W., Richardson, D. C. 2002. Formation of Asteroid Families by Catastrophic Disruption: Simulations with Fragmentation and Gravitational Reaccumulation. *Icarus* 160, 10-23.
- Morbidelli, A., Bottke, W. F., Froeschlé, C., and Michel, P. 2002. Origin and Evolution of Near-Earth Objects. *Asteroids III*, 409-422.
- Morbidelli, A., Nesvorný, D., Bottke, W. F., Michel, P., Vokrouhlický, D., and Tanga, P. 2003. The shallow magnitude distribution of asteroid families. *Icarus* 162, 328-336.
- Nesvorný, D., Bottke, W. F., Dones, L., Levison, H. F. 2002. The recent breakup of an asteroid in the main-belt region. *Nature* 417, 720-771.
- Nesvorný, D., Jedicke, R., Whiteley, R. J., and Ivezić, Ž. 2005. Evidence for asteroid space weathering from the Sloan Digital Sky Survey. *Icarus* 173, 132-152.
- Ostro, S. J., Campbell, D. B., Hine, A. A., Shapiro, I. I., Chandler, J. F., Werner, C. L., Rosema, K. D. 1990. Radar images of asteroid 1627 Ivar. *Astronomical Journal* 99, 2012-2018.
- Pauls, A., and Gladman, B. 2005. Decoherence Time Scales for Meteorite Streams. Submitted to *MAPS*.
- Raymond, S. N., and 23 colleagues 2004. A Strategy for Finding Near-Earth Objects with the SDSS Telescope. *Astronomical Journal* 127, 2978-2987.
- Richardson, D. C., Bottke, W. F., and Love, S. G. 1998. Tidal Distortion and Disruption of Earth-Crossing Asteroids. *Icarus* 134, 47-76.
- Richardson, D. C., Quinn, T., Stadel, J., Lake, G. 2000. Direct Large-Scale N-Body Simulations of Planetesimal Dynamics. *Icarus* 143, 45-59.
- Smirnov, N. 1933. Estimate of deviation between empirical distribution functions in two independent samples. *Bull. Moscow Univ.* 2 (2) 3.
- Southworth, R. B., Hawkins, G. S. 1963. Statistics of meteor streams. *Smithsonian Contributions to Astrophysics* 7, 261.
- Tanga, P., Cellino, A., Michel, P., Zappalà, V., Paolicchi, P., dell'Oro, A. 1999. On the Size Distribution of Asteroid Families: The Role of Geometry. *Icarus* 141, 65-78.
- Valsecchi, G. B., Joepk, T. J., Froeschle, C. 1999. Meteoroid stream identification: a new approach - I. Theory. *Monthly Notices of the Royal Astronomical Society* 304, 743-750.
- Veeder, G. J., Hanner, M. S., Matson, D. L., Tedesco, E. F., Lebofsky, L. A., Tokunaga, A. T. 1989. Radiometry of near-earth asteroids. *Astronomical Journal* 97, 1211-1219.
- von Mises, R. 1964. *Mathematical Theory of Probability and Statistics* (New York: Academic Press), Chapters IX(C) and IX(E).
- Stephens, M. A., 1970, *Journal of the Royal Statistical Society, ser. B*, vol. 32, pp. 115-122.
- Zappalà, V., Cellino, A., dell'Oro, A., and Paolicchi, P. 2002. Physical and Dynamical Properties of Asteroid Families. *Asteroids III* 619-631.

Number	Name	Designation	H	Tax.	Effective Diameter (km) ($p_V = 0.306$)	Effective Diameter (km) ($p_V = 0.128$)	Effective Diameter (km) ($p_V = 0.070$)
1627	Ivar		13.2	S	5.50	8.50	11.50
5836		1993 MF	13.9	S	3.98	6.16	8.33
2368	Beltrovata		15.21	SQ	2.18	3.37	4.56
3102	Krok		15.6	S	1.82	2.81	3.81
13553		1992 JE	16.0		1.51	2.34	3.17
12923		1999 GK4	16.1	S	1.45	2.24	3.02
39796		1997 TD	16.3		1.32	2.04	2.76
		1998 KU2	16.61	F,Cb	1.14	1.77	2.39
10860		1995 LE	17.3		0.83	1.29	1.74
8034	Akka		17.9	S,Q	0.63	0.98	1.32
27031		1998 RO4	17.9		0.63	0.98	1.32
65996		1998 MX5	18.06	X	0.59	0.91	1.23
		1987 SF3	18.69		0.44	0.68	0.92
8014		1990 MF	18.7		0.44	0.68	0.91
		1989 RC	18.75		0.43	0.66	0.89
		1991 RJ2	19.15		0.36	0.55	0.74
		1998 MR24	19.15		0.36	0.55	0.74
26310		1998 TX6	19.2	C	0.35	0.54	0.73
		1972 RB	19.24		0.34	0.53	0.71
		1998 ME3	19.25	F	0.34	0.52	0.71
26817		1987 QB	19.5		0.30	0.47	0.63
		1997 RT	19.8	O	0.26	0.41	0.55
		1994 TA2	20.31		0.21	0.32	0.44
		1998 QQ52	20.89		0.16	0.25	0.33
		1995 SA4	22.26		0.08	0.13	0.18
Lower limit →					6.37 km	9.84 km	13.31 km

TABLE 1

THE A1 ASSOCIATION OF DRUMMOND (2000) IN ORDER OF INCREASING ABSOLUTE MAGNITUDE (H). THIS IS THE LARGEST ASSOCIATION IDENTIFIED WITHIN THE NEO POPULATION KNOWN AT THE TIME. OUR NOMINAL VALUES FOR THE ASSUMED DIAMETERS OF THE OBJECT CORRESPOND TO THE INTERMEDIATE ALBEDO VALUE OF $p_V = 0.128$.

Grouping (Fu et al.)	Members	Association (Drummond 2000)	Members	Overlap
1	29	A1	25	25
2	23	A8	11	11
3	23	A4	10	9
4	22	A2	15	15

TABLE 2

A COMPARISON BETWEEN THE FOUR LARGEST ASSOCIATIONS IDENTIFIED IN THIS ANALYSIS AND IN DRUMMOND (2000). THE FOUR LARGEST GROUPS FOUND IN THIS ANALYSIS CONTAIN FOUR OF THE ASSOCIATIONS IDENTIFIED BY DRUMMOND (2000).

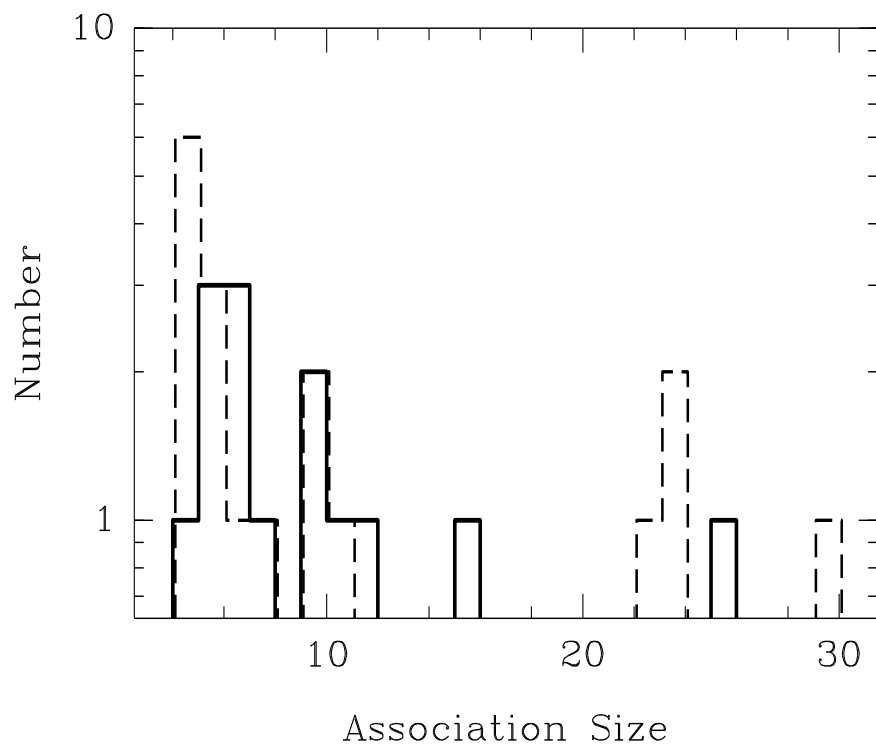


FIG. 1.— Size distribution of associations published in Drummond (2000) (solid line) and the associations detected by the volume search code of this analysis (dashed line).

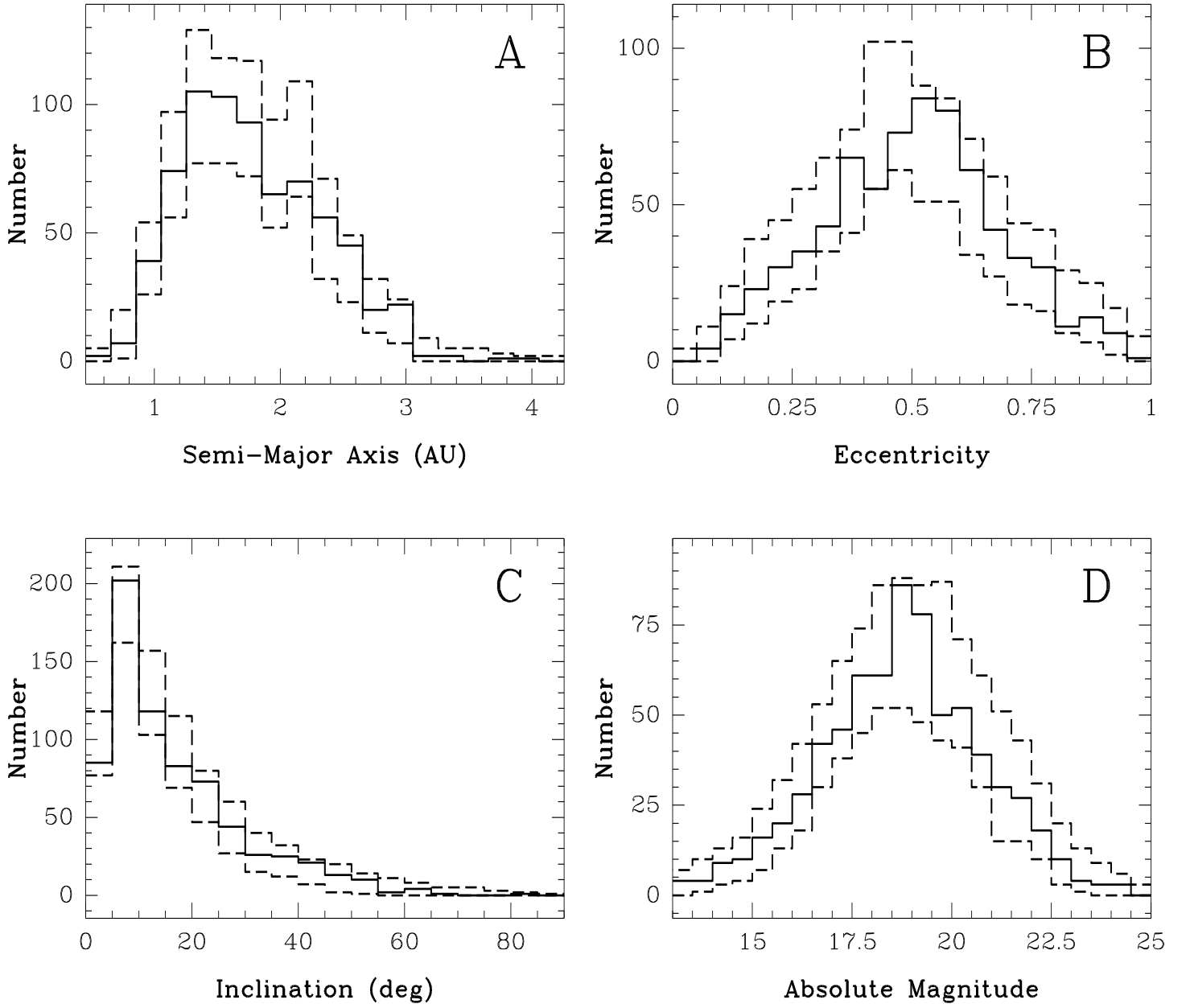


FIG. 2.— Minimum and maximum (lower and upper dashed lines respectively) distribution of 100 synthetic observed NEO populations designed to model the distribution of NEOs known at the time of Drummond's (2000) study (solid line). A) semi-major axis B) eccentricity C) inclination D) absolute magnitude.

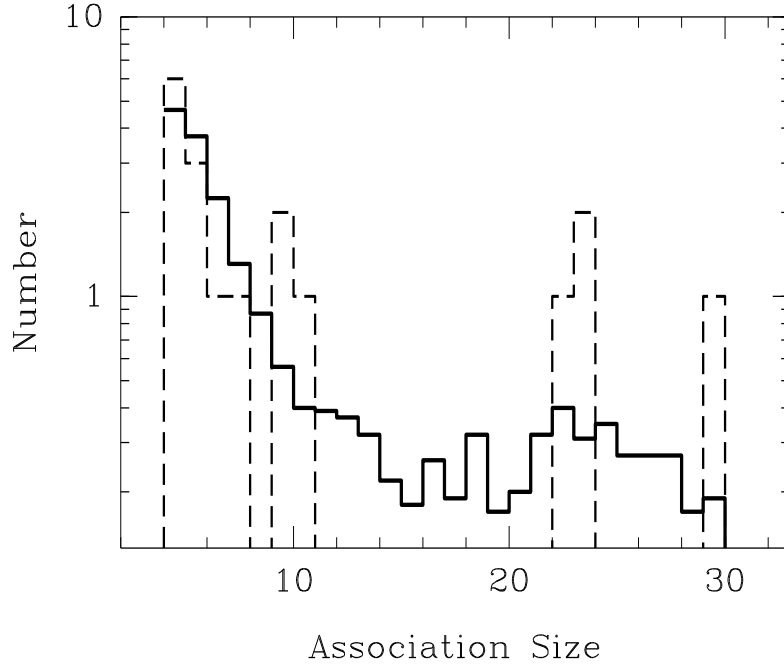


FIG. 3.— Average size distribution of associations detected from 100 synthetic NEO populations (solid line) and the distribution of associations found in this analysis in the same sample as used in Drummond (2000) (dashed line).

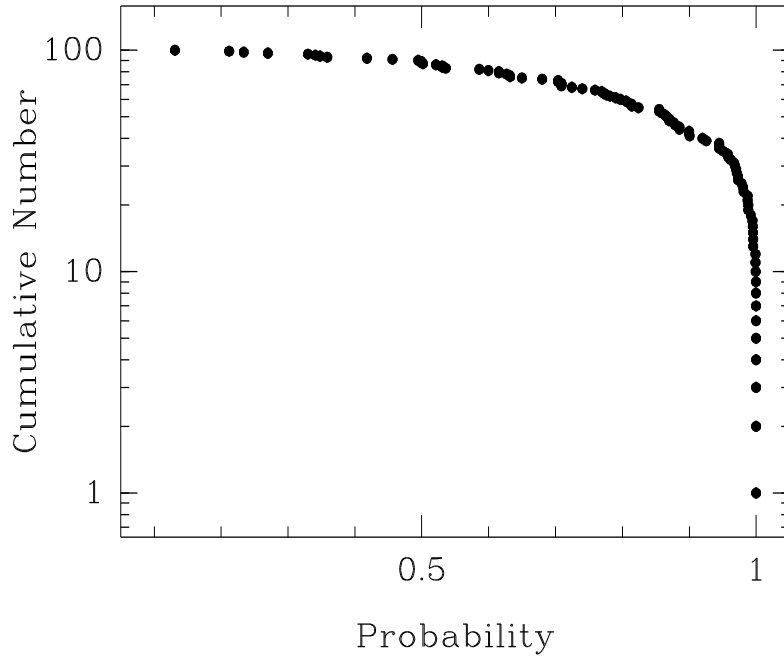


FIG. 4.— Cumulative distribution of the Kolmogorov-Smirnov probability that the size distribution of associations found in a synthetic NEO population and the one from the actual NEO population are consistent. For example, at a confidence level $\gtrsim 90\%$, the size distributions of associations detected in ~ 40 of the 100 synthetic NEO populations are statistically consistent with the same distribution found in the actual NEO population.

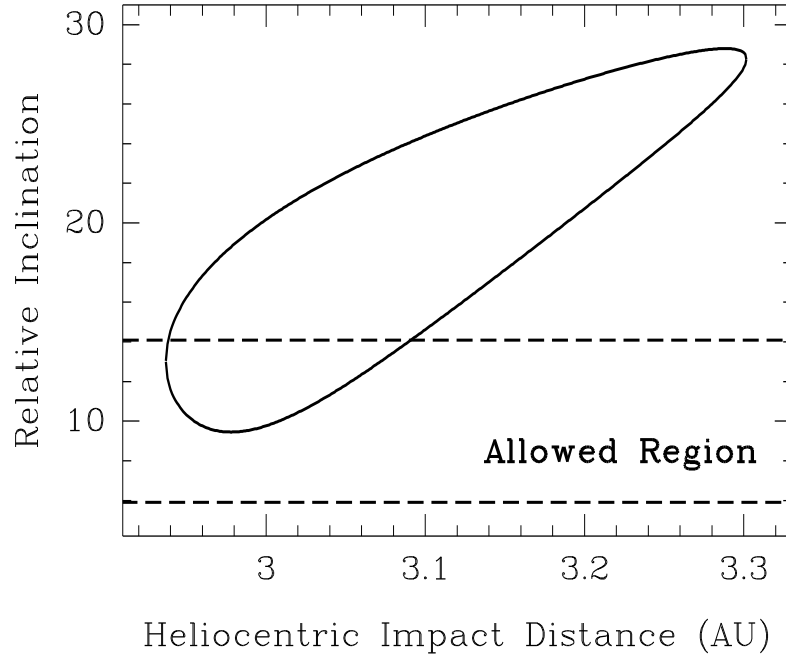


FIG. 5.— Relative inclination vs. heliocentric impact distance for the A1 precursor and projectile (see text for details). The loop shows the relative inclinations required in order to provide the relative impact speed (8.36 km/s) as a function of the heliocentric impact distance. The area bracketed by the dashed lines indicates the region of possible relative inclinations between the A1 precursor and the projectile, *i.e.*, smaller than the sum of and bigger than the difference between their orbit inclinations.

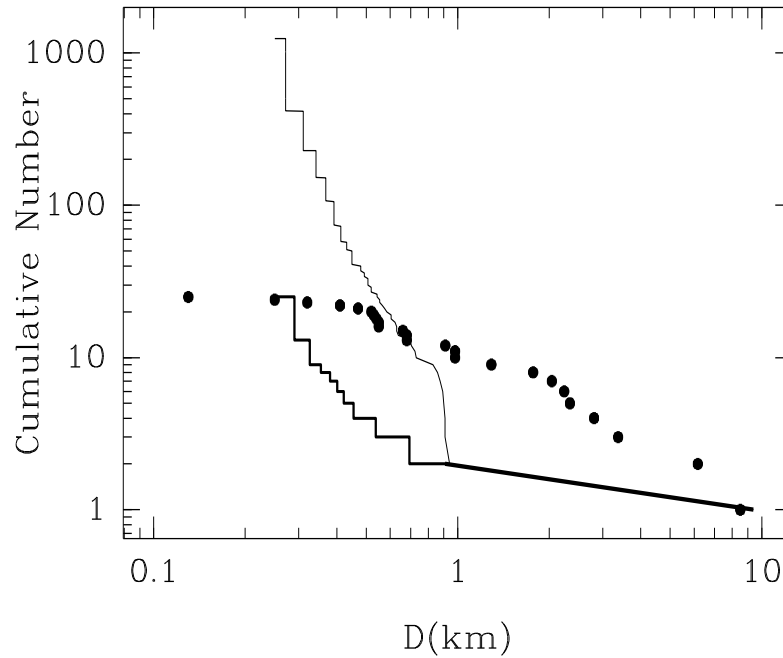


FIG. 6.— Cumulative size distribution of the actual A1 association (dots) and the synthetic A1-like family before (thin line) and after (thick line) applying an *ad hoc* observational selection effect.

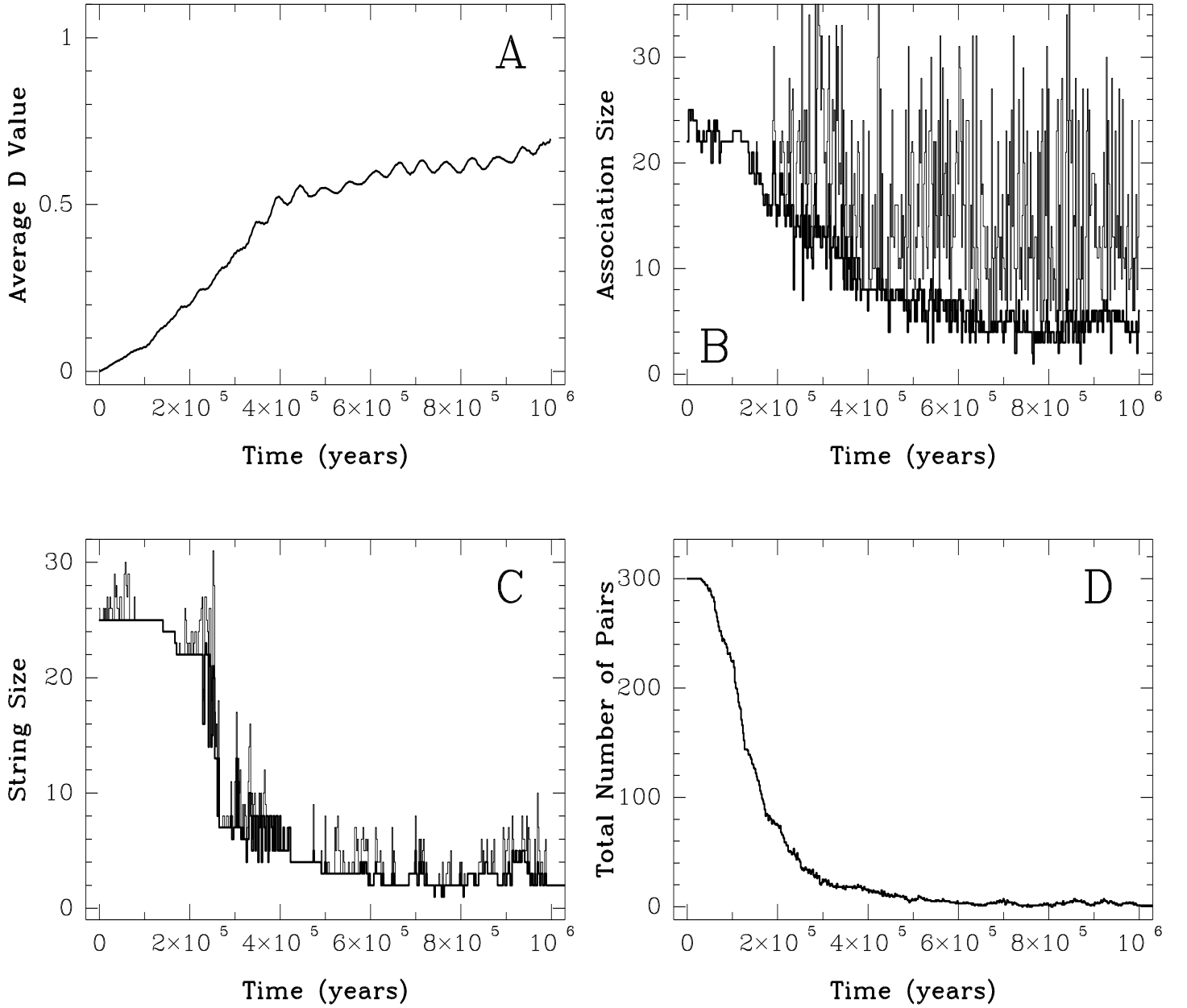


FIG. 7.— Evolution of a synthetic A1-like association in the next 1 Myr. These results use the B1 background population and an impact heliocentric distance of 2.98 AU for the collision (see text for details). A) the mean D -criterion value among all synthetic A1 members, B) the largest detectable A1-like *association* (thin line) and the number of objects that are original members of the synthetic family (thick line) in each detected group, C) the largest *string* with $D_{string} = 0.1$ (thin line) and the number of objects that are original members of A1 (thick line), D) total number of all *pairs* within the original synthetic A1 members meeting the $D_{pair} = 0.1$ threshold.

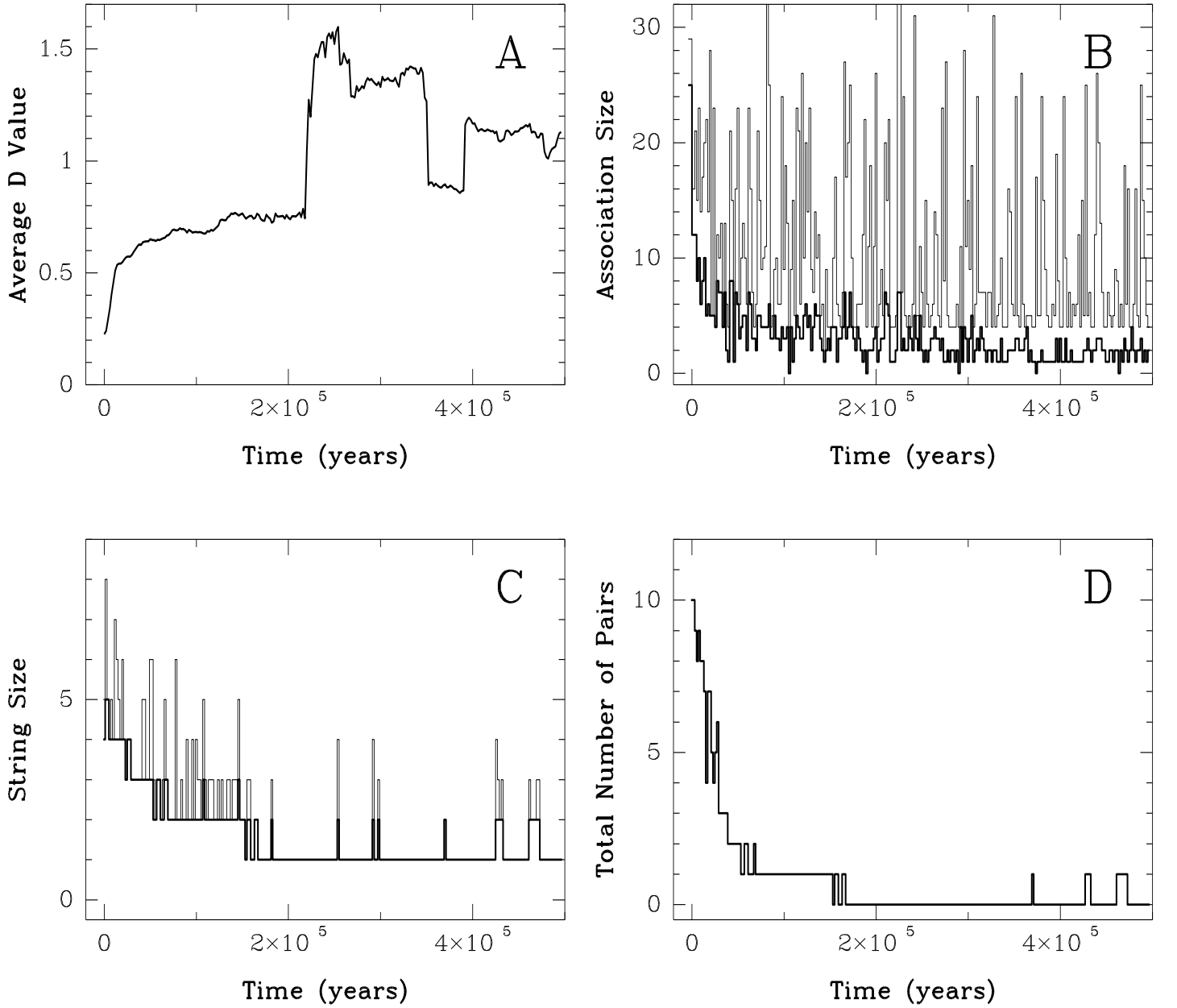


FIG. 8.— Evolution of Drummond's (2000) A1 association in the next 500 Kyr — The sub-figures are otherwise identical in description to those in Fig. 7 but are reproduced here for clarity. A) the mean D -criterion value among all original A1 members, B) the largest detectable A1-like *association* (thin line) and the number of objects that are original A1 members detected in each detected group (thick line), C) the largest *string* with $D_{string} = 0.1$ (thin line) and the number of objects that are members of the original A1 association (thick line), D) total number of all *pairs* amongst the original A1 members meeting the $D_{pair} = 0.1$ threshold. There are a total of 300 ($C_{25}^2 = 25 \times 24/2$) possible pairs within the 25-member A1 association.

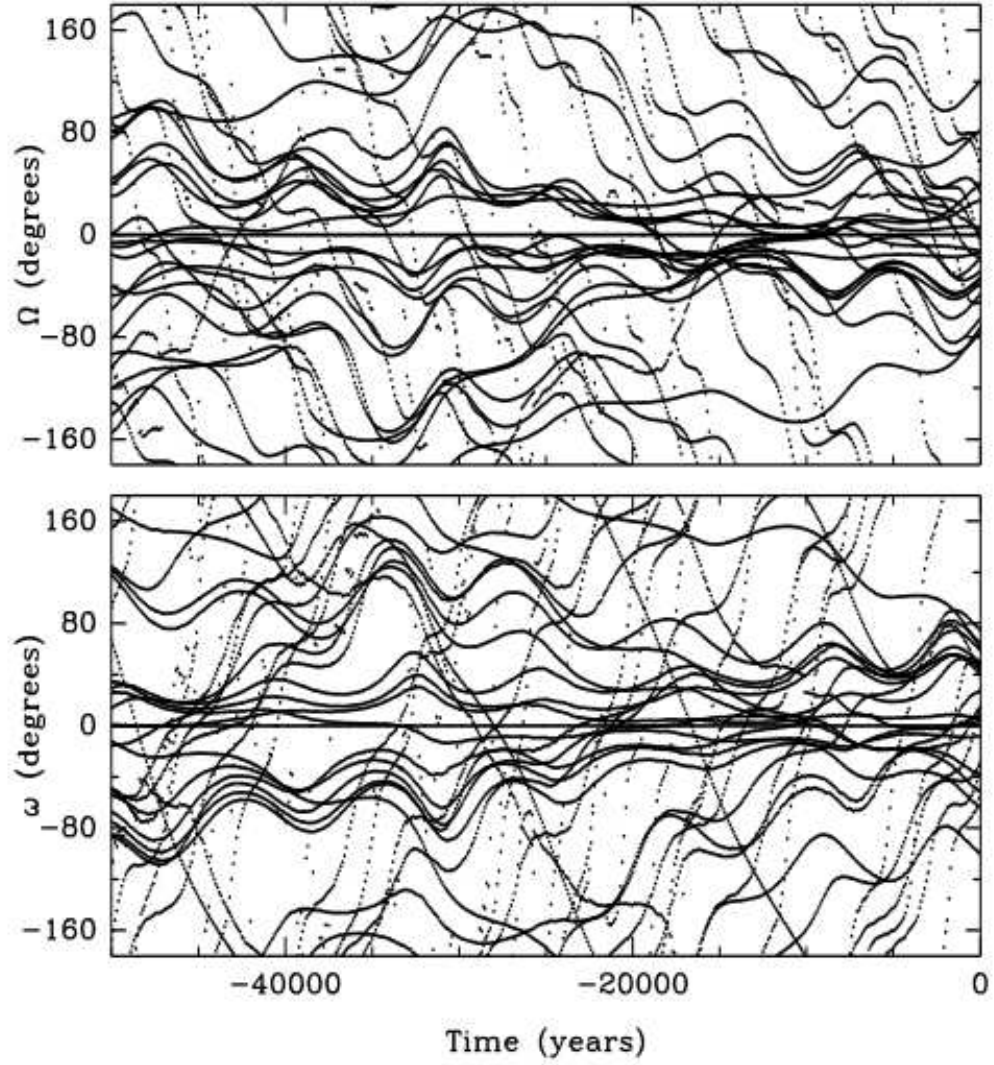


FIG. 9.— Time evolution of the longitude of the ascending node, Ω (top), and of the argument of perihelion, ω (bottom), for the 25 members of Drummond's (2000) A1 association. The orbital elements are shown relative to the value for 1998 QQ52 (that appears as the straight line at 0°) because its orbit is the closest to A1's mean orbit.

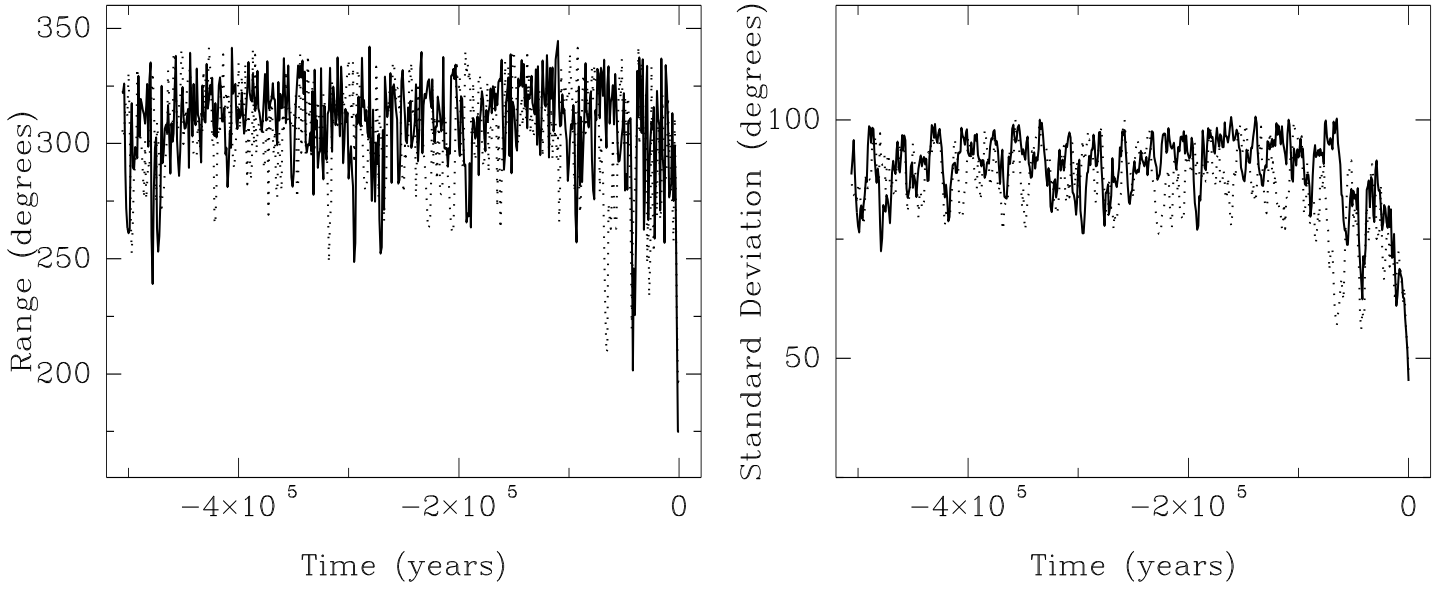


FIG. 10.— *Left* – evolution of the range (max – min) of Ω (dotted) and ω (solid) in the last 500 Kyr for Drummond's (2000) A1 association. *Right* – evolution of the RMS spread of the same angular elements. In creating these figures we have taken into account the wrap-around at the $360^\circ \rightarrow$ boundary.

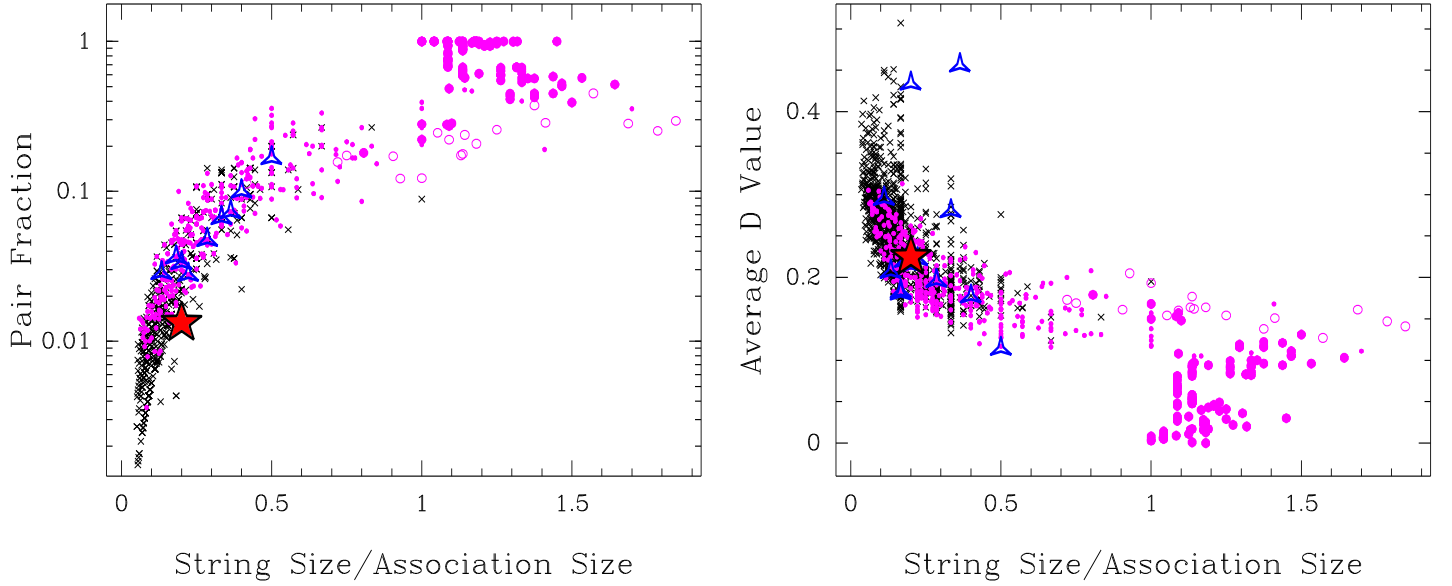


FIG. 11.— *Left* – pair fraction vs. string and association size ratio diagram. *Right* – average D -criterion value vs. string and association size ratio diagram. Large magenta solid dots — associations detected between $T = 0$ and 210 Kyr; large magenta circles — associations detected between $T = 210$ Kyr and 250 Kyr; small magenta dots — associations detected after 250 Kyr; black crosses – associations detected in the synthetic NEO populations; red star — current location of Drummond's (2000) A1 association; blue open triangles — current locations of Drummond's (2000) associations A2 – A14.